A correspondence between the Rabi model and an Ising model with long-range interactions

Bruno Scheihing-Hitschfeld[1⋆] and Néstor Sepúlveda[2†]

1 Kavli Institute for Theoretical Physics, University of California, Santa Barbara, California 93106, USA
2 School of Engineering and Sciences, Universidad Adolfo Ibáñez, Diagonal las Torres 2640, Peñalolen, Santiago, Chile

⋆ bscheihi@kitp.ucsb.edu , † nesepulv@gmail.com

Abstract

By means of Trotter's formula, we show that transition amplitudes between a class of generalized coherent states in the Rabi model can be understood in terms of a certain Ising model featuring long-range interactions beyond nearest neighbors in its thermodynamic limit. Specifically, we relate the transition amplitudes in the Rabi model to a sum over binary variables of the form of a partition function of an Ising model with a number of spin sites equal to the number of steps in Trotter's formula applied to the real-time evolution of the Rabi model. From this, we show that a perturbative expansion in the energy splitting of the two-level subsystem in the Rabi model is equivalent to an expansion in the number of spin domains in the Ising model. We conclude by discussing how calculations in one model give nontrivial information about the other model, and vice versa, as well as applications and generalizations this correspondence may find.

1   Introduction

When two apparently distinct physical theories can be shown to be equivalent, there is an opportunity to understand more deeply the inner workings of both theories, especially when the regimes in which each theory is tractable correspond to values of the parameters/couplings that are intractable from the point of view of the other theory. Fundamental dualities across different areas of physics reveal deep connections between seemingly distinct frameworks. In quantum mechanics, the Fourier transform formalizes the position-momentum duality [1,2], showing that a system's description in position space is mathematically equivalent to its representation in momentum space, directly tied to the wave-particle duality [3–5], where quantum entities exhibit both wave-like and particle-like behavior depending on observation. In statistical mechanics, the Kramers-Wannier duality [6,7] in the Ising model relates high-temperature and low-temperature regimes, offering insights into phase transitions. In condensed matter and quantum field theory, bosonization [8–11] establishes an equivalence between fermionic and bosonic descriptions in (1+1) dimensions, simplifying the study of interacting fermions. At the interface of gravity and quantum field theory, the AdS/CFT correspondence [12–14] provides a striking example of holographic duality, equating a higher-dimensional gravitational theory to a conformal field theory on its lower-dimensional boundary, offering profound insights into quantum gravity and strongly coupled systems. These dualities not only facilitate calculations but also deepen our conceptual understanding of physical phenomena.

In all of these examples, it is possible to formulate physical questions in one theory and answer them using the machinery of the other, equivalent description. Some observables that may be very difficult to calculate in one description may be simple in the other, and vice-versa.

In this work, by means of Trotter's formula [15] applied to real-time quantum evolution, we show that there exists a correspondence between the quantum mechanical transition amplitudes of the Rabi model [16,17] and the partition function of a specific 1D Ising model [18] with nonlocal interactions. That is to say, we show that the dynamics of a quantum theory may be understood in terms of the partition function of a higher-dimensional theory with a different set of degrees of freedom, and vice-versa. We also show how to cast this correspondence in imaginary time, allowing for well-developed methods in statistical physics to have direct applicability.

On the one hand, the Rabi model is a theory of interest as a model of the interaction

of electromagnetic waves with an atom in a cavity. In a unit system where $\hbar = 1$, the
Hamiltonian can be expressed as

$$\mathcal{H} = \omega_0 \sigma^z + \omega a^\dagger a + g \sigma^x (a + a^\dagger) , \tag{1}$$

where a, $a^\dagger$ represent the annihilation and creation operators of a photon of frequency ω,
and σ^k with $k \in \{x, y, z\}$ are the Pauli matrices, modeling the atom in the cavity as a two-
level system with an energy splitting of ω_0. Lastly, the term proportional to g describes
interactions between the two sectors of the theory.

The Rabi model has been extensively studied across various regimes. It is often
solved using the Rotating Wave Approximation (RWA), which is valid near resonance
when counter-rotating terms oscillate much faster than rotating terms and can be ne-
glected, leading to the well-known Jaynes-Cummings model [19]. This simplification en-
ables analytical solutions and experimental confirmation revealing quantum effects such
as collapse and revival of atomic inversion [20, 21], spontaneous emission, and absorp-
tion [19, 22].

However, the RWA's validity depends on the coupling ratio g/ω. While it holds in
the strong coupling regime ($g/\omega < 0.1$), it breaks down in the ultra-strong ($g/\omega \geq 0.1$)
and deep strong coupling ($g/\omega > 1$) regimes, even at exact resonance [23–28].

While these extreme regimes are challenging to achieve in quantum-optical cavity
quantum electrodynamics (QED), circuit QED offers tunable couplings that allow counter-
rotating terms to generate novel quantum effects beyond the predictions of the RWA
[23–25]. These effects include ultrastrong coupling state engineering and tomography
[29], sub-cycle switching of ultrastrong light-matter interactions [30], Bloch-Siegert fre-
quency shifts [31, 32], and violations of selection rules leading to unconventional transi-
tions [33].

From a theoretical perspective, solutions for its energy levels and eigenfunctions have
been obtained in terms of transcendental functions related to Heun functions [34]. And
while much is understood about the theory, it is not too difficult to encounter quantities
for which more tools would be desirable. Consider preparing the photons in a "classical"
coherent state $|\alpha\rangle_c$, characterized by $a |\alpha\rangle_c = \alpha |\alpha\rangle_c$. A natural question to ask is how
this state evolves when interacting with the two-level system via Eq. (1), which we can
characterize by calculating

$$\mathcal{A}_{s'\beta,s\alpha} = \left\langle s', \beta \right|_c e^{-i\mathcal{H}t} |s, \alpha\rangle_c = \left\langle s', \beta \right|_c U(t) |s, \alpha\rangle_c , \tag{2}$$

where $U(t)$ represents the time evolution operator and s, s' the eigenvalues of σ^z.

In this work, we will derive a formula to calculate a family of directly related am-
plitudes – which may in fact be used to reconstruct Eq. (2) – without solving a differen-
tial equation. We will do so in terms of a set of generalized coherent states, defined as
eigenstates of spin-dependent annihilation operators $b \equiv \sigma^x a$ and a parity operator Π,
introduced later in the text. For brevity, we will denote these generalized states simply
by $|\alpha\rangle$ by working in a fixed parity sector, with the understanding that they differ from
the usual coherent states of a (denoted, as above, by $|\alpha\rangle_c$). Explicit formulas and further
details of these states are provided in Appendix A, where the parity operator Π and the
photon-atom entanglement structure of these states are discussed at length.

The formula we will derive is nothing else than the partition function of an Ising
model.

The Ising model is one of the oldest and most well-studied systems in physics. It con-
sists of a chain of spins, each taking values of $+1$ or, -1 which interact with their nearest
neighbors. The system evolves to minimize its energy, often leading to an ordered (ferro-
magnetic) or disordered (paramagnetic) phase, depending on temperature and external

102 fields. However, despite of its ubiquitousness, these spin chains can be as complex as the
103 interactions between the individual sites.

104   The form that we will consider in this work is

$$\mathcal{H}_{\text{Ising}} = -\sum_{i,j} \sigma_i^z K_{i,j} \sigma_j^z - \sum_i \sigma_i^z B_i \,, \tag{3}$$

105 where σ_i^z is the Pauli matrix in the z-direction representing a spin at site i, $K_{i,j}$ represents
106 the interactions between spins, and B_i a local magnetic field that favors one orientation
107 over the other. From a quantum mechanical point of view, there is nothing complicated
108 about this model: its eigenstates are simply products of the eigenstates of each Pauli
109 matrix σ_i^z, and the energy of each state is obtained by evaluating the sum in Eq. (3) for
110 a given spin configuration. However, any calculation with it will, in principle, be as
111 complicated as the interaction matrix $K_{i,j}$. One quantity of interest in such a model is its
112 partition function, as it encodes the thermodynamic properties of the spin chain. Taking
113 the trace over the basis of eigenstates (for simplicity, in units where $k_B T = 1$), one obtains

114

$$Z = \sum_{\{s_i\}_{i=1}^N} \exp\left(\frac{1}{2}\sum_{i,j} s_i K_{i,j} s_j + \sum_i s_i B_i\right) \,, \tag{4}$$

115 for which there is no simple, closed expression unless more information is given on K and
116 B such that the sum may be carried out. We will show that a sum of this form determines
117 the value of the amplitude (8).

118   In what follows, two steps are necessary to make this connection: to recast the anni-
119 hilation and creation operators a, $a^\dagger$ in terms of $b \equiv \sigma^x a$ and $b^\dagger \equiv \sigma^x a^\dagger$. The advantage of
120 doing this is that the Rabi Hamiltonian takes the form

$$\mathcal{H} = -\omega_0 e^{i\pi b^\dagger b}\Pi + \omega b^\dagger b + g(b^\dagger + b) \,, \tag{5}$$

121 where $\Pi = -e^{i\pi a^\dagger a}\sigma^z = -e^{i\pi b^\dagger b}\sigma^z$ is a parity operator, i.e., it has discrete eigenvalues
122 $P = \pm 1$, and it commutes with $\mathcal{H}$, meaning that we may simply replace Π by its eigen-
123 value when studying the dynamics of the system. By doing this, we have reduced the
124 problem to one set of creation and annihilation operators, satisfying the usual commuta-
125 tion relations $[b, b^\dagger] = 1$, and whose action on a state do not mix different parity subsec-
126 tors: $\Pi b \Pi = b$. The eigenstates of a and b are nonetheless related to each other by taking
127 appropriate linear combinations. For example,

$$|P = -1, \alpha\rangle = \frac{1}{2}\left(|+, \alpha\rangle_c + |+, -\alpha\rangle_c + |-, \alpha\rangle_c - |-, -\alpha\rangle_c\right) \,, \tag{6}$$

$$|+, \alpha\rangle_c = \frac{1}{2}\left(|P = -1, \alpha\rangle + |P = -1, -\alpha\rangle + |P = +1, \alpha\rangle - |P = +1, -\alpha\rangle\right) \,. \tag{7}$$

128 That is to say, the amplitudes expressed in the b basis can be fully re-expressed in terms
129 of the original a operators by superimposing states from the two parity operator Π eigen-
130 vector subspaces. Eqs. (6) and (7) are two examples of how the coherent states defined
131 by $b = \sigma^x a$ can be written as linear combinations of a-coherent states with fixed spin
132 states and vice-versa. The rest of these relations are listed in Appendix A. These iden-
133 tities demonstrate explicitly that knowledge of overlaps in the b basis is equivalent to
134 knowledge of overlaps in the a basis.

135   Therefore, our object of interest in this work, which fully characterizes (albeit indi-
136 rectly) the amplitude in Eq. (2), is

$$\mathcal{A}_{\beta\alpha} = \langle\beta| e^{-i\mathcal{H}t} |\alpha\rangle = \langle\beta| U(t) |\alpha\rangle \,, \tag{8}$$

137 where we have suppressed the parity label, as we do throughout the rest of the text.

2 Trotter's formula and the real-time correspondence

The other ingredient we need in order to make this connection is Trotter's formula [15].
Let's assume we start with an arbitrary generalized coherent state $|\alpha\rangle$, characterized by
$b|\alpha\rangle = \alpha|\alpha\rangle$. To find the evolution of this state in time, let us define

$$\mathcal{H} = \mathcal{H}_1 + \mathcal{H}_2 + \mathcal{H}_3 \tag{9}$$

with $\mathcal{H}_1 = -P\omega_0 e^{i\pi b^\dagger b}$, $\mathcal{H}_2 = \omega b^\dagger b$ and $\mathcal{H}_3 = g(b^\dagger + b)$. Finding the action of $U(t)$ is not
trivial since $\mathcal{H}_1$ and $\mathcal{H}_2$ do not commute with $\mathcal{H}_3$. However, we can use Trotter's formula

$$U(t) = \lim_{n\to\infty}(e^{-i\mathcal{H}_1 t/n}e^{-i\mathcal{H}_2 t/n}e^{-i\mathcal{H}_3 t/n})^n \tag{10}$$

to make progress.

Let U_n be defined as

$$U_n = e^{-i\lambda_n b^\dagger b}e^{-i\delta_n e^{i\pi b^\dagger b}}e^{\gamma_n(b^\dagger + b)}, \tag{11}$$

where $\lambda_n = \omega t/n$, $\delta_n = -P\omega_0 t/n$ and $\gamma_n = -igt/n$. One can then apply U_n n times over
the state $|\alpha\rangle$ to calculate its time evolution. It follows that

$$e^{\gamma_n(b^\dagger + b)}|\alpha\rangle = e^{\gamma_n Re(\alpha)}|\alpha + \gamma_n\rangle, \tag{12}$$

$$e^{-i\delta_n e^{i\pi b^\dagger b}}|\alpha\rangle = \cos\delta_n|\alpha\rangle - i\sin\delta_n|-\alpha\rangle, \tag{13}$$

$$e^{-i\lambda_n b^\dagger b}|\alpha\rangle = \left|e^{-i\lambda_n}\alpha\right\rangle, \tag{14}$$

and therefore, that

$$U_n|\alpha\rangle = e^{\gamma_n Re(\alpha)}\left[\cos\delta_n\left|(\alpha + \gamma_n)e^{-i\lambda_n}\right\rangle - i\sin\delta_n\left|-(\alpha + \gamma_n)e^{-i\lambda_n}\right\rangle\right]. \tag{15}$$

That is to say, each step in the Trotterized evolution of the state includes a continuous
action on the state plus a splitting mediated by the interaction proportional to ω_0.

We can then consider the transition amplitudes between coherent states. Using Trotter's formula in Eq. (8), these are given by

$$\mathcal{A}_{\beta\alpha} = \langle\beta|U(t)|\alpha\rangle = \lim_{n\to\infty}\langle\beta|U_n^n|\alpha\rangle. \tag{16}$$

From the structure of the previous equation it is clear that the Trotterized amplitude
$\langle\beta|U_n^n|\alpha\rangle$ at a fixed n will contain 2^n terms. Furthermore, each action of U_n modifies
the components of the state by flipping the sign of the eigenvalue of b. It should therefore not come as a surprise that this sum of 2^n terms may be written in terms of a sum
over the possible configurations of n sign variables $s_i \in \{-1, 1\}$, with $i = 1, \ldots, n$. That is
to say, a sum like the one that appears in the partition function of the Ising model.

Indeed, using results from Appendices B and C, in Appendix D we show that

$$\lim_{n\to\infty}\langle\beta|U_n^n|\alpha\rangle = \lim_{n\to\infty}\left(\frac{-i\sin(2\delta_n)}{2}\right)^{n/2}e^{-\frac{|\alpha|^2+|\beta|^2}{2}}\left\{\sum_{\substack{\{s_k\}_{k=1}^{n-1}\\s_0=s_n=1}}e^{\frac{1}{2}\sum_{j,\ell=1}^{n-1}s_j s_\ell K_{j,\ell}+\sum_{\ell=1}^{n-1}s_\ell B_\ell^+ + e^{-i\omega t}\beta^*\alpha}\right.$$

$$\left. + \sum_{\substack{\{s_k\}_{k=1}^{n-1}\\s_0=-s_n=1}}e^{\frac{1}{2}\sum_{j,\ell=1}^{n-1}s_j s_\ell K_{j,\ell}+\sum_{\ell=1}^{n-1}s_\ell B_\ell^- - e^{-i\omega t}\beta^*\alpha}\right\} \tag{17}$$

where

$$K_{j,\ell} = \delta_{\ell,j+1} \ln(i \cot \delta_n) + \gamma_n^2 e^{-i|j-\ell|\lambda_n}, \tag{18}$$

$$B_\ell^\pm = \gamma_n \left[\beta^* e^{-i\ell\lambda_n} \pm \alpha e^{-i(n-\ell)\lambda_n} \right]. \tag{19}$$

Note that $\delta_{\ell,j+1}$ in Eq. (18) denotes a Kronecker delta, ensuring that the logarithmic term contributes only when $\ell = j + 1$. These expressions have exactly the structure of the partition function of an Ising model, with the important feature that several quantities are complex (as is necessary for this formulation to reproduce a quantum mechanical amplitude). This is our first main result.

In practice, calculating these amplitudes directly in the Rabi model becomes increasingly expensive at large values of α and β, since one must numerically represent a Hilbert space large enough to accommodate the coherent states $|\alpha\rangle$ and $|\beta\rangle$. Exact diagonalization methods require a cutoff $N_{\max}$ on the photon number basis, with $N_{\max}$ typically scaling as $|\alpha|^2$ to achieve convergence, because the Poissonian weight $p_N = e^{-|\alpha|^2}|\alpha|^{2N}/N!$ extends up to $N \approx |\alpha|^2$. By contrast, our mapping avoids this: it relies on the partition function of an associated Ising model and thus does not require explicit overlaps with a truncated bosonic basis. In our approach, the cost is completely contained within the time evolution. In particular, the Trotter discretization converges with a number of time slices n that scales linearly with $|\alpha|$ (see Appendix B.2). As we discuss in the next section in terms of an expansion in the number of "domain walls" of the partition function, and in more generally in Appendix B.2, this can lead to more efficient calculations than the Hilbert space truncation.

We close this section by noting that this expression may be rewritten in terms of imaginary time $\tau = it$ to make the closest connection with well-developed methods of statistical physics. We discuss this further in Section 4.

3 The continuum limit of the Ising model as a perturbative expansion in ω_0

Given that the full amplitude $\langle\beta| U(t) |\alpha\rangle$ in Eq (17) is given by a limit, it is natural to ask if there is an explicit way to take the limit. Viewed as a spin chain, all of the terms in Eqs. (18) and (19) have a straightforward continuum limit because the $1/n$ factor in γ_n converts the sums into Riemann sums that converge to integrals, except for the nearest neighbor terms controlled by δ_n.

In the continuum limit $n \to \infty$, the magnitude $\ln|\cot\delta_n|$ grows without bound, meaning it is energetically favorable to have as few sign flips as possible. It then becomes natural to organize the sum over the sign variables as a function of the number of sign flips in the sequence $\{s_i\}$. Let m be that number. In the continuum limit, the position of the individual sign flips $\{i_k\}_{k=1}^m$ may be characterized by uniform random variables $z_k \in [0,1]$, each one corresponding to the value of i_k/N.

Following through with this rearrangement, we may take the limit $n \to \infty$ at each fixed value of m and obtain a series expression for $\langle\beta| U(t) |\alpha\rangle$. We show details of this derivation in Appendix D. We obtain

$$\langle\beta|U(t)|\alpha\rangle = e^{-\frac{|\alpha|^2 - 2\beta^*\alpha + |\beta|^2}{2}} e^{\frac{ig^2 t}{\omega}} \sum_{m=0}^{\infty} \frac{(iP\omega_0 t)^m}{m!} e^{-\frac{2mg^2}{\omega^2} - \left(\alpha + \frac{g}{\omega}\right)\left(\beta^* + \frac{g}{\omega}\right)\left[1-(-1)^m e^{-i\omega t}\right]} F_m, \tag{20}$$
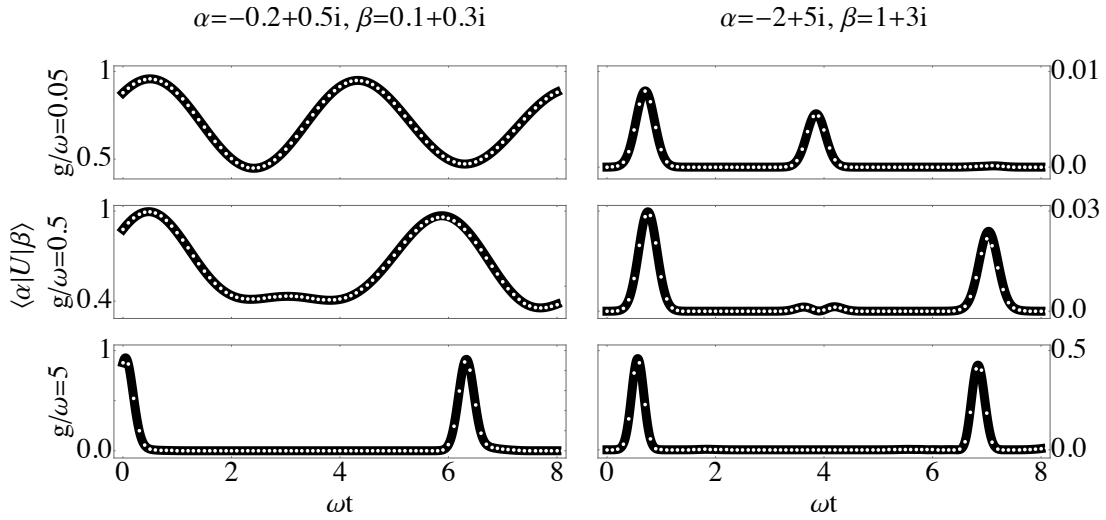
Figure 1: Transition amplitudes between two pairs of generic coherent states: $|\alpha\rangle = |-0.2 + 0.5i\rangle$ and $|\beta\rangle = |0.1 + 0.3i\rangle$ (first column), and $|\alpha\rangle = |-2 + 5i\rangle$ and $|\beta\rangle = |1 + 3i\rangle$ (second column), considering parity equal to +1. The black curves represent the numerical solution of the Schrödinger equation for the Rabi Hamiltonian, while the white dotted curves correspond to Eq. (20) with $m_{\mathrm{max}} = 10$ and 10^4 sampling steps for each value of m from 1 to m_{max} to compute the mean value and obtain F_m using Eq. (21). For a given value of m, which represents the number of domain walls (or spin flips) in the spin chain Hamiltonian, a sampling step corresponds to the random assignment of spin flip positions along the chain, independently distributed within the interval $(0, 1)$. In all plots we used $\omega_0/\omega = 0.3$. We compare both results across three coupling regimes: strong coupling ($g/\omega = 0.05$, first row), ultra-strong coupling ($g/\omega = 0.5$, second row), and deep strong coupling ($g/\omega = 5$, third row).

where F_m is given by

$$
F_m = \left\langle \exp\left(-\frac{4g^2}{\omega^2} \sum_{k=1}^{m} \sum_{\ell=1}^{k-1} (-1)^{k+\ell} e^{-i(z_k - z_\ell)\omega t} - \frac{2g}{\omega} \sum_{k=1}^{m} \left[\left(\beta^* + \frac{g}{\omega}\right)(-1)^k e^{-iz_k \omega t} \right. \right. \right.
$$
$$
\left. \left. \left. - \left(\alpha + \frac{g}{\omega}\right)(-1)^{m+k} e^{-i(1-z_k)\omega t} \right] \right) \right\rangle_m .
$$
(21)

The average $\langle \cdot \rangle_m$ is taken over the possible sign flip positions $z_k \in (0, 1)$ (the "domain wall" positions in the spin chain), with $\{z_k\}_{k=1}^{m}$ an ordered sequence. Explicitly,

$$
\langle G \rangle_m = m! \int_0^1 dz_m \int_0^{z_m} dz_{m-1} \ldots \int_0^{z_2} dz_1 \, G(z_1, z_2, \ldots, z_m) .
$$
(22)

Eq. (20) is our second main result.

It is clear from Eq. (20) that the result of taking the continuum limit in this form yields a perturbative expansion in ω_0, of the same form that one would get using time-dependent perturbation theory. While on the one hand the limit $n \to \infty$ has been taken, the convergence of the series requires more and more terms as t grows larger, and each coefficient of the series (which are also time-dependent) requires one to evaluate averages for which we have not found a closed form, meaning that the practical applicability

of this formula is not obviously superior to the one given earlier in Eq. (17). However, it provides one with another, independent handle to calculate the transition amplitudes.

Figure 1 presents a comparison of the numerical solution of the Schrödinger equation for the Rabi Hamiltonian with Eq. (20) across the three previously mentioned regimes: strong coupling, ultra-strong coupling, and deep strong coupling. It is important to emphasize that Eq. (20) was derived from Eq. (17), and that the interpretation in terms of a Ising model is still transparent: m is the number of "domain walls" (or sign flips) in the spin chain Hamiltonian defined by Eq. (17).

It is worth emphasizing that in going from Eq. (17) to Eq. (20), m is always smaller than n, meaning that the information encoded in the first n terms of Eq. (17) is contained within the first n terms of Eq. (20). Taken together with the estimate in Appendix B.2, this suggests that to stay below an error tolerance ε, one needs $m \gtrsim C_1 g\omega|\alpha|t^2/\varepsilon$, scaling linearly with α. However, inspecting Eq. (20), we see that this might be an overly conservative estimate, as the result is organized as a power series in $\omega_0 t$, while the sensitivity to α, β is purely contained in the integral moments F_m. In particular, a scan over the values of ω_0 could be done (up to a given tolerance fixed by the value of $\omega_0 t$) at significantly lower cost than with a direct diagonalization approach if one calculates the functions F_m in advance.

All the results presented so far correspond to the real-time dynamics of the Rabi model. The derivation based on Trotter's formula and the mapping to the effective Ising chain, as well as the continuum-limit expansion in Eq. (20), have all been carried out in real time, preserving the unitary time evolution of the quantum system. This distinguishes our approach from the usual imaginary-time (Euclidean) formulations, which are typically used to study equilibrium properties. In contrast, our construction explicitly captures the coherent dynamics and interference effects, such as the revival phenomena observed in Fig. 1, which are intrinsic features of the real-time quantum evolution.

4 Applications in imaginary time

We now look at likely applications of this correspondence beyond the calculation of amplitudes just described, first starting from calculations on the Ising model side, and then commenting on the converse direction. We focus on imaginary time applications, as real partition functions are natural objects to calculate from the Ising side of the correspondence.

4.1 What this Ising model can do for the Rabi model

We begin by considering the imaginary time version of the amplitudes $\langle \beta | U(t) | \alpha \rangle$. It is not hard to see that upon substituting $\tau = it$, the formula for the amplitudes is given by

$$
\langle \beta | U | \alpha \rangle = \lim_{n \to \infty} \left(\frac{\sinh(2P\omega_0\tau/n)}{2} \right)^{n/2} e^{-\frac{|\alpha|^2 + |\beta|^2}{2}} \left\{ \sum_{\substack{\{s_k\}_{k=1}^{n-1} \\ s_0 = s_n = 1}} e^{\frac{1}{2}\sum_{j,\ell=1}^{n-1} s_j s_\ell K_{j,\ell}^E + \sum_{\ell=1}^{n-1} s_\ell B_\ell^{E+} + e^{-\omega\tau}\beta^*\alpha} \right.
$$

$$
\left. + \sum_{\substack{\{s_k\}_{k=1}^{n-1} \\ s_0 = -s_n = 1}} e^{\frac{1}{2}\sum_{j,\ell=1}^{n-1} s_j s_\ell K_{j,\ell}^E + \sum_{\ell=1}^{n-1} s_\ell B_\ell^{E-} - e^{-\omega\tau}\beta^*\alpha} \right\}
$$

(23)

where

$$K_{j,\ell}^{E} = \delta_{\ell,j+1} \ln\left(\coth\frac{P\omega_0\tau}{n}\right) + \frac{g^2\tau^2}{n^2}e^{-|j-\ell|\omega\tau/n} , \tag{24}$$

$$B_{\ell}^{E\pm} = -\frac{g\tau}{n}\left[\beta^* e^{-\ell\omega\tau/n} \pm \alpha e^{-(n-\ell)\omega\tau/n}\right] . \tag{25}$$

It is instructive to analyze more closely the form of the Ising couplings in Eq. (24). The kernel $K_{j,\ell}^{E}$ has two contributions: (i) a nearest–neighbor term $\delta_{\ell,j+1}\ln(\coth(P\omega_0\tau/n))$, which plays the role of a strong coupling between consecutive time slices in the Trotter decomposition, effectively enforcing that the spin configuration does not fluctuate arbitrarily from one slice to the next and thus depends on ω_0, and (ii) a ferromagnetic, exponentially decaying tail $\frac{g^2\tau^2}{n^2}e^{-|j-\ell|\omega\tau/n}$ whose amplitude grows with g^2 and whose range is set by ω. In the continuum limit, this second contribution becomes a non-local interaction kernel proportional to $e^{-\omega\tau|u-v|}$ with $u = j/n$, $v = \ell/n$. Taking the Fourier transform of this long-range part alone shows that its spectral weight has the form $\widetilde{K}(k) \propto [(\omega\tau)^2 + k^2]^{-1}$, i.e. a Yukawa-type kernel. This Fourier representation is not used in the subsequent calculations, but it is useful to highlight the effective range and structure of the induced interactions on the Ising side.

This structure reveals how different dynamical regimes of the Rabi model appear on the Ising side. For weak coupling $g \ll \omega, \omega_0$, the long–range piece is negligible and the dynamics is dominated by the short–range stiffness. Conversely, in the ultra-strong and deep-strong coupling regimes $g \sim \omega$ or $g \gg \omega$, the ferromagnetic tail becomes long-ranged and sizable, strongly suppressing domain walls in imaginary time. This behavior encodes the crossover between perturbative dynamics and the strongly correlated regime, providing an explicit Ising–side diagnostic of the dynamical phases of the Rabi model.

The case where $\alpha = \beta = 0$ is a particularly simple instance of this formula, which we will revisit in the next section. In this case we simply have

$$\langle 0|U|0\rangle = \lim_{n\to\infty}\left(\frac{\sinh(2P\omega_0\tau/n)}{2}\right)^{n/2}\sum_{\substack{\{s_k\}\\s_0=1}}e^{\frac{1}{2}\sum_{j,\ell=1}^{n-1}s_js_\ell K_{j,\ell}^{E}} , \tag{26}$$

which is to say, it takes the form of an Ising model with long-range interactions in the absence of external fields.

Even though so far the only partition function we have discussed is that of the Ising model, starting from our expressions, it happens to be quite simple to derive a formula for the partition function of the Rabi model itself, which we will denote by $\mathcal{Z}$. Specifically, one can use the completeness relation

$$\mathbb{1} = \frac{1}{\pi}\int d^2\alpha|\alpha\rangle\langle\alpha| \tag{27}$$

to calculate the trace of the time evolution operator

$$\frac{1}{2\pi}\int d^2\alpha\,\langle\alpha|U|\alpha\rangle = \sum_n e^{-E_n\tau} \equiv \mathcal{Z} \tag{28}$$

where we identify the right hand side as the partition function of the Rabi Hamiltonian (in one of its parity subsectors) where $\tau = 1/T$ is the inverse temperature of the system. We emphasize that these imaginary-time amplitudes are not only of formal interest:

They yield the finite-temperature partition function of the Rabi model (determined by the next three equations), from which physical quantities can be extracted as with any other partition function. It can also serve as a starting point for the calculation of correlation functions in imaginary time, which provides access to linear-response properties, making the amplitudes physically meaningful quantities beyond the mapping itself. Starting from Eq. (23), setting $\beta = \alpha$, carrying out the integral over α and proceeding as before to take the limit $n \to \infty$, one finds that

$$\mathcal{Z} = \sum_n e^{-E_n \tau} = \sum_{m=0}^{\infty} \frac{(\tau P \omega_0)^m}{m!} \frac{\mathcal{Z}_m}{1 - (-1)^m e^{-\tau \omega}} \tag{29}$$

where

$$\mathcal{Z}_m = \left\langle \exp \left(L[\bar{s}](\tau) + \frac{(-1)^m e^{-\tau \omega}(L[\bar{s}](\tau) + L[\bar{s}](-\tau))}{2(1 - (-1)^m e^{-\tau \omega})} \right) \right\rangle_m , \tag{30}$$

and we have introduced

$$L[\bar{s}](\tau) = -\frac{4g^2}{\omega^2} \sum_{k=1}^{m} \sum_{\ell=1}^{k-1} (-1)^{k+\ell} e^{-(z_k - z_\ell)\omega \tau} - \frac{2g^2}{\omega^2} \sum_{k=1}^{m} (-1)^k \left[e^{-z_k \omega \tau} - (-1)^m e^{-(1-z_k)\omega \tau} \right]$$

$$- \frac{g^2}{\omega^2} \left(1 - (-1)^m e^{-\omega \tau} \right) - \frac{2mg^2}{\omega^2} + \frac{g^2 \tau}{\omega} . \tag{31}$$

At large imaginary times $\tau \to \infty$ (corresponding to small temperatures), this expression is certainly more complicated than $e^{-E_0 \tau}$. However, at moderate or small values of τ, when all states contribute to the sum over eigenstates $\sum_n e^{-E_n \tau}$, Eq. (29) provides an explicit expression that avoids having to diagonalize a matrix of arbitrarily large dimension.

4.2   What the Rabi model can do for this Ising model

Although the Ising model obtained here is a specific instance thereof, with couplings determined by those of the Rabi model, we emphasize that partition functions like the ones we just encountered do appear in other contexts. For example, they share structural features with long-range interacting spin systems that naturally arise in cavity and waveguide QED [35]. The mapping therefore has relevance beyond a formal exercise, as it highlights a class of interactions of direct physical interest.

In particular, given that we know the Schrödinger equation that the quantum system satisfies, we can use it to obtain results for the partition function of the Ising model we described above. Concretely, the solution to the imaginary time Schrödinger equation

$$\partial_\tau |\psi\rangle = -\mathcal{H} |\psi\rangle , \tag{32}$$

with an initial condition specified by $|\psi(t = 0)\rangle = |\alpha\rangle$, automatically returns the thermodynamic limit $n \to \infty$ of the partition function on the RHS of Eq. (23) by calculating its overlap at time τ with the state $\langle \beta|$.

If one knows the spectrum of $\mathcal{H}$ with enough precision to calculate the decomposition of a given generalized coherent state $|\alpha\rangle$ in terms of its eigenstates $|n\rangle$, then it is natural to write

$$\langle \beta| U |\alpha\rangle = \sum_n e^{-E_n \tau} \langle \beta|n\rangle \langle n|\alpha\rangle , \tag{33}$$

meaning that the sums in Eq. (23) may be decomposed in terms of a sum of decaying exponentials, thus providing an organizing principle to evaluate them at large values of τ.

This last expression is most useful at values of α, β where only a small number of states $|n\rangle$ contribute to their decomposition in terms of eigenstates of $\mathcal{H}$. This will be the case, for example, when g/ω is small and $\alpha = \beta = 0$.

To close, we note that one relatively simple result of this correspondence is that the Ising model partition function we mentioned at the end of the last section can be written as

$$\lim_{n\to\infty} \left(\frac{\sinh(2P\omega_0\tau/n)}{2} \right)^{n/2} \sum_{\substack{\{s_k\} \\ s_0=1}} e^{\frac{1}{2}\sum_{j,\ell=1}^{n-1} s_j s_\ell K_{j,\ell}^E} = \sum_n e^{-E_n\tau} |\langle 0|n\rangle|^2 \,, \tag{34}$$

meaning that one can calculate the continuum limit of the spin system with no "magnetic fields" we described above by calculating the overlaps between the harmonic oscillator vacuum and the eigenstates of the Rabi Hamiltonian.

5 Conclusions and Outlook

We have calculated the transition amplitudes between generalized coherent states (eigenstates of $b = a\sigma_x$ and the parity operator Π) in the Rabi model and found a remarkable correspondence with the partition functions of a family of Ising models with long-range interactions. These partition functions provide explicit expressions that converge to the Rabi model amplitudes when the continuum limit is taken. The key step in the derivation was to use Trotter's formula to study the dynamics of the Rabi model, by which the parameter n that controls the number of steps in the Trotterized evolution ultimately becomes the number of sites in the "dual" Ising model. We have verified that our results reproduce the full quantum dynamics of the system, and discussed selected applications in which our expressions provide a more direct route to calculate a given observable than diagonalizing the Rabi Hamiltonian directly. This perspective highlights the broader relevance of our approach and clarifies how the effective Ising couplings reflect the different dynamical regimes of the Rabi model.

An interesting next step would be to consider other quantum mechanical models with transition amplitudes (or other quantities) that admit a dual description in terms of a spin system. While it includes highly nonlocal interactions, the fact that we obtained an alternate way of calculating the partition function of a quantum mechanical system by evaluating a partition function of a spin system in one higher dimension is very reminiscent of dualities between quantum systems and gravitational systems (e.g., the matrix model dual to Jackiw-Teitelboim gravity [36]), although further study would be required to determine whether a notion of "bulk" and "boundary" can be established as in holographic dualities.

In principle, the present method could also be applied to the limit $\omega/\omega_0 \to 0$, where the Rabi model undergoes a superradiant phase transition characterized by the spontaneous buildup of a macroscopic photon field [37] (see also [38]). Within our Ising correspondence, this regime maps onto a situation where the effective long-range kernel $K_{j,\ell}^E$ strongly suppresses domain walls, favoring globally ordered spin configurations. We expect that in this spin representation, the onset of the superradiant phase would correspond to the development of a nonzero magnetization — analogous to having a finite coherent amplitude in the bosonic description. Speculatively, the exponential decay of the kernel would suppress domain walls sufficiently to stabilize ordered phases such that it would mirror the emergence of superradiance in the Rabi model as $\omega/\omega_0 \to 0$. Although this lies beyond our present scope, our Ising formulation offers a framework

353 to investigate this superradiant limit from a complementary angle.

354 Another avenue worth exploring using our results is the many-body physics of cav-
355 ity and waveguide QED. Under various conditions, the dynamics of atom-light interac-
356 tions can be described in terms of spin chains with long-range interactions [35], where
357 their respective Hamiltonians are not at all unlike the Ising model expression we de-
358 rived, as the long-range interactions in these spin chains are mediated by couplings
359 $K_{i,j} \propto \exp(-\lambda|i - j|)$, where λ may be imaginary or real and positive. The fact that this is
360 exactly the form of the long-range interactions in the real- and imaginary-time versions
361 of the coherent to coherent state transition amplitudes, Eq. (17) and Eq. (23), respectively,
362 may open an interesting pathway to connect the dynamics of light coupled to a single
363 atom with that of light interacting with a lattice of atoms, and therefore draw far-reaching
364 lessons about the many-body physics of cavity and waveguide QED by studying a com-
365 paratively simpler quantum mechanical system.

Acknowledgements

367 The authors sincerely thank Juan Carlos Retamal for highlighting the significance of the
368 Rabi model, José Chesta-Lopez for insightful discussions during the early stages of this
369 research, and Carla Hermann-Avigliano for providing experimental information on the
370 three regimes of the Rabi model. The authors also thank the referees for their constructive
371 comments and suggestions, which helped improve the clarity and scope of this work.

372 **Funding information**   The work of BSH was supported in part by a CONICYT Grant
373 Number CONICYT- PFCHA/MagísterNacional/2018-22181513, by grant NSF PHY-2309135
374 to the Kavli Institute for Theoretical Physics (KITP), and by grant 994312 from the Simons
375 Foundation. NS was supported in part by Fondecyt grant No. 1220536 and the Millen-
376 nium Science Initiative Program NCN2024_068 of ANID, Chile.

A   Hamiltonian Model

378 We start with the Rabi model for the interaction of a quantum two-level atom with pho-
379 tons

$$\mathcal{H} = \omega_0 \sigma^z + \omega a^\dagger a + g(\sigma^+ + \sigma^-)(a^\dagger + a). \tag{A.1}$$

380 Here, the σ operators are the Pauli Matrices acting on the two level system with basis
381 $|+\rangle$ and $|-\rangle$, and $a^\dagger$ and a are the creation and annihilation operators for the photon
382 spectrum, with basis $|n\rangle$. The energy is tuned by the parameters ω_0, ω and g, representing
383 the energies of the atom levels gap, the photon frequency, and the interaction energy
384 respectively. We have set $\hbar = 1$.

385 Expanding the interaction term we obtain

$$\mathcal{H} = \omega_0 \sigma^z + \omega a^\dagger a + g(\sigma^+ a + \sigma^- a^\dagger + \sigma^+ a^\dagger + \sigma^- a). \tag{A.2}$$

386 A common approach would be to neglect the counter-rotating terms, $\sigma^+ a^\dagger + \sigma^- a$, in
387 favor of the rotating terms, $\sigma^+ a + \sigma^- a^\dagger$, by invoking the rotating wave approximation
388 (RWA). Here we analyze the problem without employing this approximation.

389 We first begin by making a transformation to the Hamiltonian, mapping it into a
390 photon system with a definite parity. Let the parity operator be

$$\Pi = -e^{i\pi a^\dagger a} \sigma^z. \tag{A.3}$$

If we take the basis $\{|s, n\rangle\}$, with $s = \pm 1$ representing the possible states of the atom, we see that the parity acts over this basis as

$$\Pi |s, n\rangle = -e^{i\pi a^\dagger a} \sigma^z |s, n\rangle = -s(-1)^n |s, n\rangle . \tag{A.4}$$

On the other hand, taking the target basis of the transformation $\{|P, n\rangle\}$, with $P = \pm 1$ representing the even and odd parities, we see that

$$\Pi |P, n\rangle = P |P, n\rangle . \tag{A.5}$$

We see that when the atom it's in the excited state ($s = 1$), the parity is odd when the photon number is even, and vice-versa. Conversely, when the atom it's in the ground state ($s = -1$), the parity is odd when the photon number is odd, and vice-versa. In conclusion, we can make a one-to-one correspondence between the $|s, n\rangle$ and the $|P, n\rangle$ bases.

With this transformation, the Hamiltonian is

$$\mathcal{H} = -\omega_0 e^{i\pi a^\dagger a} \Pi + \omega a^\dagger a + g(\sigma^+ + \sigma^-)(a^\dagger + a). \tag{A.6}$$

The elegancy of this transformation is that the system dynamics moves inside the Hilbert space split in two unconnected subspaces or parity chains

$$|-, 0_a\rangle \leftrightarrow |+, 1_a\rangle \leftrightarrow |-, 2_a\rangle \leftrightarrow |+, 3_a\rangle \leftrightarrow \ldots (P = +1), \tag{A.7}$$
$$|+, 0_a\rangle \leftrightarrow |-, 1_a\rangle \leftrightarrow |+, 2_a\rangle \leftrightarrow |-, 3_a\rangle \leftrightarrow \ldots (P = -1). \tag{A.8}$$

Neighboring states within each parity chain may be connected via either rotating or counter-rotating terms. For example, in the parity chain with $P = +1$, the counter-rotating term $\sigma^+ a^\dagger$ induces the transition $|-, 2_a\rangle \to |+, 3_a\rangle$, while the rotating term $\sigma^+ a$ induces $|+, 1_a\rangle \leftarrow |-, 2_a\rangle$.

The natural follow up question is if the basis $\{|P, n\rangle\}$ are eigenstates of the system. Clearly, since the interaction terms change the photon number the answer is no. We can see this explicitly

$$\mathcal{H} |P, n\rangle = [-\omega_0 (-1)^n P + \omega n] |P, n\rangle + g\sqrt{n+1} |P, n+1\rangle + g\sqrt{n} |P, n-1\rangle . \tag{A.9}$$

Altough the basis $\{|P, n\rangle\}$ is not an eigenenergy basis, we do conclude that the Hamiltonian is parity invariant. Therefore, in the following we will assume a fixed parity of the system and focus on only diagonalizing one of the disconnected Hilbert subspaces. With this assumption, the Hamiltonian is

$$\mathcal{H} = -\omega_0 e^{i\pi a^\dagger a} P + \omega a^\dagger a + g(\sigma^+ + \sigma^-)(a^\dagger + a). \tag{A.10}$$

Note that $\sigma^\pm, a, a^\dagger$ are defined on the full Hilbert space, not only on the fixed parity subspace. Given that we will focus on a fixed parity sector, and in order to eliminate this redundancy and simplify the calculation, we can make another canonical transformation to simplify the description of the system to a single set of creation and annihilation operators, without any spin variables remaining. Concretely, let $b = \sigma^x a$ and $b^\dagger = \sigma^x a^\dagger$. With this transformation $b^\dagger b = a^\dagger a$, therefore the photon number interpretation is not changed. Furthermore, the action of $b, b^\dagger$ does not take the state outside of the fixed parity subspace because $\Pi b \Pi = b$. The Hamiltonian follows as

$$\mathcal{H} = -\omega_0 e^{i\pi b^\dagger b} P + \omega b^\dagger b + g(b^\dagger + b). \tag{A.11}$$

Finally, we note that the coherent states with eigenvalue α associated with b are related to the ones associated with a via

$$|P = -1, \alpha\rangle = \frac{1}{2} \left(|+, \alpha\rangle_c + |+, -\alpha\rangle_c + |-, \alpha\rangle_c - |-, -\alpha\rangle_c \right) , \tag{A.12}$$

$$|P = +1, \alpha\rangle = \frac{1}{2} \left(|-, \alpha\rangle_c + |-, -\alpha\rangle_c + |+, \alpha\rangle_c - |+, -\alpha\rangle_c \right) , \tag{A.13}$$

$$|+, \alpha\rangle_c = \frac{1}{2} \left(|P = -1, \alpha\rangle + |P = -1, -\alpha\rangle + |P = +1, \alpha\rangle - |P = +1, -\alpha\rangle \right) , \tag{A.14}$$

$$|-, \alpha\rangle_c = \frac{1}{2} \left(|P = +1, \alpha\rangle + |P = +1, -\alpha\rangle + |P = -1, \alpha\rangle - |P = -1, -\alpha\rangle \right) . \tag{A.15}$$

B Trotterized time evolution of a coherent state

In the following section we will study the time evolution generated by the Hamiltonian in Eq. (A.11). To do this, we will consider a generalized coherent state

$$|\alpha\rangle_\pm = e^{-\frac{|\alpha|^2}{2}} \sum_{k=0}^{\infty} \frac{\alpha^k}{\sqrt{k!}} |P = \pm 1, k\rangle , \tag{B.1}$$

and to save space we will adopt the notation

$$|\alpha\rangle = e^{-\frac{|\alpha|^2}{2}} \sum_{k=0}^{\infty} \frac{\alpha^k}{\sqrt{k!}} |k\rangle . \tag{B.2}$$

Let's assume we start with an arbitrary coherent state $|\alpha\rangle$. The question to answer is: how does this state evolve in time? Therefore, we need to find the action of $U(t) = e^{-i\mathcal{H}t}$ over the state. Let the Hamiltonian be

$$\mathcal{H} = \mathcal{H}_1 + \mathcal{H}_2 + \mathcal{H}_3 \tag{B.3}$$

with $\mathcal{H}_1 = -\omega_0 e^{i\pi b^\dagger b} P$, $\mathcal{H}_2 = \omega b^\dagger b$ and $\mathcal{H}_3 = g(b^\dagger + b)$. Finding the action of $U(t)$ is not trivial since $\mathcal{H}_1$ and $\mathcal{H}_2$ do not commute with $\mathcal{H}_3$.

B.1 Trotter's Formula

For $U(t) = e^{-i(\mathcal{H}_1 + \mathcal{H}_2 + \mathcal{H}_3)t}$ we can use Trotter's formula

$$U(t) = \lim_{n \to \infty} (e^{-i\mathcal{H}_1 t/n} e^{-i\mathcal{H}_2 t/n} e^{-i\mathcal{H}_3 t/n})^n . \tag{B.4}$$

Let U_n be defined as

$$U_n = e^{-i\lambda_n b^\dagger b} e^{-i\delta_n e^{i\pi b^\dagger b}} e^{\gamma_n(b^\dagger + b)} , \tag{B.5}$$

where $\lambda_n = \omega t/n$, $\delta_n = -P\omega_0 t/n$ and $\gamma_n = -igt/n$. We will apply U_n, n times over the state $|\alpha\rangle$ to calculate the time evolution. Then, the operator $D(\gamma_n) = e^{\gamma_n(b^\dagger + b)}$ is a displacement operator (since γ_n is a pure imaginary) and we readily know its action over the state

$$e^{\gamma_n(b^\dagger + b)} |\alpha\rangle = D(\gamma_n) |\alpha\rangle = D(\gamma_n) D(\alpha) |0\rangle = D(\gamma_n + \alpha) e^{(\gamma_n \alpha^* - \gamma_n^* \alpha)/2} |0\rangle . \tag{B.6}$$

Since γ_n is purely imaginary

$$e^{\gamma_n(b^\dagger + b)} |\alpha\rangle = e^{\gamma_n \mathrm{Re}(\alpha)} D(\gamma_n + \alpha) |0\rangle = e^{\gamma_n \mathrm{Re}(\alpha)} |\alpha + \gamma_n\rangle . \tag{B.7}$$

441   Next, we want to know the action of $e^{-i\delta_n e^{i\pi b^\dagger b}}$ over a state $|\alpha\rangle$

$$
\begin{aligned}
e^{-i\delta_n e^{i\pi b^\dagger b}} |\alpha\rangle &= e^{-|\alpha|^2/2} \sum_{k=0}^{\infty} \frac{\alpha^k}{\sqrt{k!}} e^{-i\delta_n e^{i\pi b^\dagger b}} |k\rangle \\
&= e^{-|\alpha|^2/2} \sum_{k=0}^{\infty} \frac{\alpha^k}{\sqrt{k!}} e^{-i\delta_n e^{i\pi k}} |k\rangle \\
&= e^{-|\alpha|^2/2} \sum_{k=0}^{\infty} \left(\frac{\alpha^{2k}}{\sqrt{(2k)!}} e^{-i\delta_n} |2k\rangle + \frac{\alpha^{2k+1}}{\sqrt{(2k+1)!}} e^{i\delta_n} |2k+1\rangle \right).
\end{aligned}
\tag{B.8}
$$

442   Let's note that the coherent states $|\alpha\rangle$ and $|-\alpha\rangle$ can be expanded as:

$$
|\alpha\rangle = e^{-|\alpha|^2/2} \left(\frac{\alpha^0}{\sqrt{0!}} |0\rangle + \frac{\alpha^1}{\sqrt{1!}} |1\rangle + \frac{\alpha^2}{\sqrt{2!}} |2\rangle + \frac{\alpha^3}{\sqrt{3!}} |3\rangle + \frac{\alpha^4}{\sqrt{4!}} |4\rangle + \cdots \right),
\tag{B.9}
$$

443

$$
|-\alpha\rangle = e^{-|\alpha|^2/2} \left(\frac{\alpha^0}{\sqrt{0!}} |0\rangle - \frac{\alpha^1}{\sqrt{1!}} |1\rangle + \frac{\alpha^2}{\sqrt{2!}} |2\rangle - \frac{\alpha^3}{\sqrt{3!}} |3\rangle + \frac{\alpha^4}{\sqrt{4!}} |4\rangle - \cdots \right).
\tag{B.10}
$$

444   Therefore,

$$
|\alpha\rangle + |-\alpha\rangle = 2e^{-|\alpha|^2/2} \sum_{k=0}^{\infty} \frac{\alpha^{2k}}{\sqrt{(2k)!}} |2k\rangle ,
\tag{B.11}
$$

445

$$
|\alpha\rangle - |-\alpha\rangle = 2e^{-|\alpha|^2/2} \sum_{k=0}^{\infty} \frac{\alpha^{(2k+1)}}{\sqrt{(2k+1)!}} |2k+1\rangle .
\tag{B.12}
$$

446   Using this we find the action of the operator

$$
\begin{aligned}
e^{-i\delta_n e^{i\pi b^\dagger b}} |\alpha\rangle &= \frac{1}{2} \left(e^{-i\delta_n}(|\alpha\rangle + |-\alpha\rangle) + e^{i\delta_n}(|\alpha\rangle - |-\alpha\rangle) \right) \\
&= \frac{e^{-i\delta_n} + e^{i\delta_n}}{2} |\alpha\rangle + \frac{e^{-i\delta_n} - e^{i\delta_n}}{2} |-\alpha\rangle \\
&= \cos\delta_n |\alpha\rangle - i\sin\delta_n |-\alpha\rangle .
\end{aligned}
\tag{B.13}
$$

447   Finally we wish to know the action of $e^{-i\lambda_n b^\dagger b}$ over a state $|\alpha\rangle$

$$
e^{-i\lambda_n b^\dagger b} |\alpha\rangle = e^{-|\alpha|^2/2} \sum_{k=0}^{\infty} \frac{\alpha^k}{\sqrt{k!}} e^{-i\lambda_n b^\dagger b} |k\rangle = e^{-|\alpha|^2/2} \sum_{k=0}^{\infty} \frac{(e^{-i\lambda_n}\alpha)^k}{\sqrt{k!}} |k\rangle = \left| e^{-i\lambda_n}\alpha \right\rangle .
\tag{B.14}
$$

448   We now can conclude, summarizing our previous derivations that

$$
U_n |\alpha\rangle = e^{\gamma_n Re(\alpha)} \left[\cos\delta_n \left| (\alpha + \gamma_n)e^{-i\lambda_n} \right\rangle - i\sin\delta_n \left| -(\alpha + \gamma_n)e^{-i\lambda_n} \right\rangle \right].
\tag{B.15}
$$

449   With this, we see that the action of one unitary operator U_n "splits" a coherent state into
450 two pieces. For n applications of U_n, we will be able to write the resulting state as a dot
451 product between coherent states and coefficients:

$$
U_n^n |\alpha\rangle = \begin{pmatrix} b_n^0 \\ b_n^1 \\ \vdots \\ b_n^{2^n-1} \end{pmatrix} \cdot \begin{pmatrix} |a_n^0\rangle \\ |a_n^1\rangle \\ \vdots \\ |a_n^{2^n-1}\rangle \end{pmatrix}.
\tag{B.16}
$$

We work this out explicitly in Appendix C, and we find that the dot product just written is explicitly determined by the functions

$$f(n, l) = \sum_{k=0}^{n-1} \lfloor l/2^k \rfloor \, , \tag{B.17}$$

$$S(n, l) = \sum_{k=1}^{n} e^{i(\pi f(k,l) - k\lambda_n)} \, , \tag{B.18}$$

$$G(l) = 1 + (-1)^l e^{2i\delta_n} \, , \tag{B.19}$$

$$H(n, l) = \frac{e^{-in\delta_n}}{2^n} \prod_{k=0}^{n-1} G(\lfloor l/2^k \rfloor) \, , \tag{B.20}$$

$$J(n, l) = \sum_{k=0}^{n-1} e^{i(\pi f(k, \lfloor l/2^{n-k} \rfloor) - k\lambda_n)} \, , \tag{B.21}$$

$$Z(n, l) = \sum_{k=0}^{n-1} S(k, \lfloor l/2^{n-k} \rfloor)) \, , \tag{B.22}$$

and reads

$$U_n^n |\alpha\rangle = \sum_{k=0}^{2^n - 1} H(n, k) e^{\gamma_n Re(\alpha J(n,k) + \gamma_n Z(n,k))} |e^{i(\pi f(n,k) - n\lambda_n)} \alpha + S(n, k)\gamma_n\rangle \, . \tag{B.23}$$

This expression completely determines the time evolution of a coherent state in this model.

Our ultimate goal would be to take the limit $n \to \infty$ of (B.23). To gain insight into how we could achieve this, we shall first examine the amplitudes implied by this expression. Specifically, coherent-to-coherent state amplitudes.

B.2 Scaling of Trotter discretization and comparison with Hilbert-space truncation

To clarify the computational scaling discussed in the main text, we analyze how the number of Trotter slices n relates to the model parameters, and compare this with the Hilbert–space cutoff N_{max} required in direct diagonalization.

In the Rabi Hamiltonian,

$$\mathcal{H} = \omega_0 \sigma^z + \omega a^\dagger a + g\sigma^x(a + a^\dagger) \, , \tag{B.24}$$

the coherent states $|\alpha\rangle$ and $|\beta\rangle$ have a Poissonian occupation distribution $p_N = \dfrac{|\alpha|^{2N} e^{-|\alpha|^2}}{N!}$ in terms of the harmonic oscillator basis (with its basis states labeled by N), which extends up to $N \approx |\alpha|^2$. Therefore, the cutoff required for numerical convergence in exact diagonalization scales as $N_{max} \sim |\alpha|^2$.

In the Trotter decomposition, time evolution is approximated as

$$e^{-it\mathcal{H}} \approx \left(e^{-i\frac{t}{n}\mathcal{H}_0} e^{-i\frac{t}{n}\mathcal{H}_{int}} \right)^n \, , \tag{B.25}$$

with a global error that scales as

$$\|e^{-it\mathcal{H}} - U_n^n\| \lesssim \frac{C_1 t^2}{n} \|[\mathcal{H}_0, \mathcal{H}_{int}]\| \, . \tag{B.26}$$

where C_1 is a numerical constant of order unity (see Refs. [39–42]). For the Rabi Hamiltonian, the dominant commutator behaves as $[\mathcal{H}_0, \mathcal{H}_{\text{int}}] \sim g\omega\sigma^x(a^\dagger - a)$, whose expectation value scales as $\|[\mathcal{H}_0, \mathcal{H}_{\text{int}}]\| \sim g\omega|\alpha|$. Requiring the Trotter error to remain below a tolerance ε gives

$$n \gtrsim C_1 \frac{g\,\omega\,|\alpha|\,t^2}{\varepsilon}. \tag{B.27}$$

Hence, while N_{max} quantifies the required Hilbert–space size, n determines the temporal resolution. Their respective dependencies, $N_{\text{max}} \sim |\alpha|^2$ and $n \propto |\alpha|$, illustrate the more favorable scaling of the Trotter–Ising formulation.

In numerical applications, the tolerance ε is typically chosen between 10^{-5} and 10^{-6} for imaginary–time simulations (see what follows) and somewhat larger (10^{-4}–10^{-5}) for real–time evolution, balancing stability and computational cost. Even with these stringent tolerances, the linear scaling of cost with n makes the Ising mapping significantly more efficient than Hilbert–space truncation approaches, which scale as $\mathcal{O}(N_{\text{max}}^2)$–$\mathcal{O}(N_{\text{max}}^3)$.

A completely analogous argument applies for imaginary time evolution. In this case the Trotter approximation is

$$e^{-\tau\mathcal{H}} \approx \left(e^{-\frac{\tau}{n}\mathcal{H}_0} e^{-\frac{\tau}{n}\mathcal{H}_{\text{int}}} \right)^n , \tag{B.28}$$

with a global error that scales as

$$\|e^{-\tau\mathcal{H}} - U_n^n\| \lesssim \frac{C_1\tau^2}{n} \, \|[\mathcal{H}_0, \mathcal{H}_{\text{int}}]\| , \tag{B.29}$$

Just like before, requiring the Trotter error to remain below a tolerance ε gives

$$n \gtrsim C_1 \frac{g\,\omega\,|\alpha|\,\tau^2}{\varepsilon} . \tag{B.30}$$

We note that even though the nature of the deviations in this case — mostly controlled by decaying exponentials — are different than in real time, where oscillatory phases appear, the same global bound applies.

This analysis thus confirms that the present formulation offers a scalable and accurate route for both real– and imaginary–time simulations of the Rabi model and related spin–boson systems.

To understand why the apparent exponential growth in configurations does not spoil this efficiency, we analyze the internal structure of the Trotter–Ising representation.

For a fixed number of slices n, the kernels $K_{j,\ell}$ and sources $B_\ell^\pm$ are oscillatory in (j, ℓ), except for the local term $\delta_{\ell,j+1}$. The suppression of most spin configurations $\{s_\ell\}$ arises not from local decay but from two mechanisms: (i) a nearest–neighbor domain–wall penalty and (ii) destructive phase interference in the long–range and linear couplings.

The complex action is

$$\mathcal{S}[s] = \frac{1}{2} \sum_{j,\ell=1}^{n-1} s_j s_\ell K_{j,\ell} + \sum_{\ell=1}^{n-1} s_\ell B_\ell^\pm, \qquad s_\ell \in \{-1, 1\}. \tag{B.31}$$

The nearest–neighbor contribution yields

$$J_n^{\text{R}} = \Re[\ln(i\cot\delta_n)] = \ln|\cot\delta_n|, \qquad J_n^{\text{E}} = \ln\left(\coth\frac{P\omega_0\tau}{n} \right) > 0. \tag{B.32}$$

For practical Trotter choices (n large), $\delta_n \ll 1$ and $J_n^{\text{R}} \simeq \ln n - \ln(P\omega_0 t) > 0$, so both real and imaginary time favor spin alignment. If m is the number of domain walls, the real

504   part of the action scales as $\Re\,\mathcal{S}_{NN}[s] \sim mJ_n$, exponentially suppressing configurations
505   with many domain walls.

506   The long–range part of the kernel in real time,

$$K_{j,\ell}^{(LR,R)} = \gamma_n^2 e^{-i|j-\ell|\lambda_n}, \tag{B.33}$$

507   contributes

$$\sum_{j,\ell} s_j s_\ell e^{-i|j-\ell|\lambda_n} = (n-1) + 2\sum_{d=1}^{n-2}\cos(d\lambda_n)\,C_d(s), \qquad C_d(s) = \sum_{j=1}^{n-1-d} s_j s_{j+d}. \tag{B.34}$$

508   Using $|C_d(s)| \le n$ and Dirichlet–kernel bounds,

$$\left|\sum_{j,\ell} s_j s_\ell e^{-i|j-\ell|\lambda_n}\right| \lesssim n + \frac{n}{|\sin(\lambda_n/2)|}, \tag{B.35}$$

509   yielding

$$\Re\left[\frac{1}{2}\gamma_n^2 \sum_{j,\ell} s_j s_\ell e^{-i|j-\ell|\lambda_n}\right] = \mathcal{O}\left(\frac{g^2 t}{\omega}\right), \tag{B.36}$$

510   which is finite and independent of n. In imaginary time, since $K_{j,\ell}^{(LR,E)} > 0$, the bound
511   improves to $\mathcal{O}((gt)^2/n)$, vanishing as $n \to \infty$.

512   The linear source term,

$$B_\ell^\pm = \gamma_n[\beta^* e^{-i\ell\lambda_n} \pm \alpha e^{-i(n-\ell)\lambda_n}], \tag{B.37}$$

513   obeys

$$\left|\sum_\ell s_\ell B_\ell^\pm\right| \le (gt)\,(|\alpha|+|\beta|), \tag{B.38}$$

514   independent of n, and tighter in imaginary time due to exponential decay.

515   Combining all contributions,

$$|e^{\mathcal{S}[s]}| \le \exp\left[mJ_n + C_1\frac{g^2 t}{\omega} + C_2(gt)(|\alpha|+|\beta|)\right], \tag{B.39}$$

516   where C_1 and C_2 are positive constants, independent of n and of order unity ($\mathcal{O}(1)$). Thus,
517   for fixed n, configurations with many domain walls are exponentially suppressed, while
518   the nonlocal and linear terms remain bounded.

519   The oscillatory structure selects spin domains of typical size $\Delta i \sim n/(\omega t)$, implying a
520   characteristic number of domain walls $m_\star \sim \omega t$, independent of n. Large $|\alpha|, |\beta|$ values
521   further stabilize these domains without changing this scaling.

522   Grouping configurations by m,

$$\sum_{m>M}\sum_{s:\#DW(s)=m} |e^{\mathcal{S}[s]}| \le e^{C_1\frac{g^2 t}{\omega}+C_2(gt)(|\alpha|+|\beta|)} \sum_{m>M}\binom{n}{m}e^{mJ_n}. \tag{B.40}$$

523   For $J_n > 0$, the tail becomes negligible for $M \gtrsim m_\star \sim \omega t$, independent of n, implying
524   polynomial computational scaling in n (and linear in M).

525   In the ω_0–expansion,

$$\left|\sum_{m>M}\frac{(iP\omega_0 t)^m}{m!}F_m\right| \le e^{C_3(gt)(|\alpha|+|\beta|)+C_4\frac{g^2 t}{\omega}}\sum_{m>M}\frac{(|P\omega_0 t|)^m}{m!}\Xi_m, \tag{B.41}$$

526 where Ξ_m bounds $|F_m|$, C_3 and C_4 are positive constants, independent of n and of order
527 unity ($\mathcal{O}(1)$). Factorial decay ensures convergence, and choosing $M \sim \omega t$ captures the
528 dominant contribution with tolerance independent of n.
529   In summary, even though the formal sum involves 2^n configurations, only $\mathcal{O}(\omega t)$ of
530 them contribute significantly due to domain–wall suppression and bounded long–range
531 interactions. Combined with the global Trotter–error bound, this shows that the Trot-
532 ter–Ising formulation achieves controlled accuracy and polynomial computational scal-
533 ing for both real– and imaginary–time evolutions.

C   Derivation of dot product formula

535 The action of one Trotterized unitary time evolution operator gave us:

$$U_n \left|\alpha\right\rangle = e^{\gamma_n Re(\alpha)} \left[\cos \delta_n \left|(\alpha + \gamma_n)e^{-i\lambda_n}\right\rangle - i \sin \delta_n \left|-(\alpha + \gamma_n)e^{-i\lambda_n}\right\rangle \right]. \tag{C.1}$$

536   Applying again, we obtain for U_n^2

$$\begin{aligned}
U_n^2 \left|\alpha\right\rangle = e^{\gamma_n Re(\alpha)} \Big\{ &\cos \delta_n e^{\gamma_n Re((\alpha+\gamma_n)e^{-i\lambda_n})} \\
&\times \Big[\cos \delta_n \left|((\alpha + \gamma_n)e^{-i\lambda_n} + \gamma_n)e^{-i\lambda_n}\right\rangle \\
&\quad - i \sin \delta_n \left|-((\alpha + \gamma_n)e^{-i\lambda_n} + \gamma_n)e^{-i\lambda_n}\right\rangle \Big] \\
&- i \sin \delta_n e^{\gamma_n Re((\alpha+\gamma_n)e^{-i\lambda_n})} \\
&\times \Big[\cos \delta_n \left|(-(\alpha + \gamma_n)e^{-i\lambda_n} + \gamma_n)e^{-i\lambda_n}\right\rangle \\
&\quad - i \sin \delta_n \left|-(-(\alpha + \gamma_n)e^{-i\lambda_n} + \gamma_n)e^{-i\lambda_n}\right\rangle \Big] \Big\},
\end{aligned} \tag{C.2}$$

537 and for U_n^3

$$\begin{aligned}
U_n^3 \left|\alpha\right\rangle = e^{\gamma_n Re(\alpha)} \Big\{ &\cos \delta_n e^{\gamma_n Re(\beta_1)} \\
&\times \Big[\cos \delta_n e^{\gamma_n Re(\beta_2)} \Big(\cos \delta_n \left|(\beta_2 + \gamma_n)e^{-i\lambda_n}\right\rangle - i \sin \delta_n \left|-(\beta_2 + \gamma_n)e^{-i\lambda_n}\right\rangle \Big) \\
&\quad - i \sin \delta_n e^{-\alpha_m Re(\beta_2)} \Big(\cos \delta_n \left|(-\beta_2 + \gamma_n)e^{-i\lambda_n}\right\rangle - i \sin \delta_n \left|-(-\beta_2 + \gamma_n)e^{-i\lambda_n}\right\rangle \Big) \Big] \\
&- i \sin \delta_n e^{-\gamma_n Re(\beta_1)} \\
&\times \Big[\cos \delta_n e^{-\gamma_n Re(\beta_2)} \Big(\cos \delta_n \left|(-\beta_2 + \gamma_n)e^{-i\lambda_n}\right\rangle - i \sin \delta_n \left|-(-\beta_2 + \gamma_n)e^{-i\lambda_n}\right\rangle \Big) \\
&\quad - i \sin \delta_n e^{\gamma_n Re(\beta_2)} \Big(\cos \delta_n \left|(\beta_2 + \gamma_n)e^{-i\lambda_n}\right\rangle - i \sin \delta_n \left|-(\beta_2 + \gamma_n)e^{-i\lambda_n}\right\rangle \Big) \Big] \Big\},
\end{aligned} \tag{C.3}$$

538 where in the last equation we have defined $\beta_1 = (\alpha + \gamma_n)e^{-i\lambda_n}$ and $\beta_2 = (\beta_1 + \gamma_n)e^{-i\lambda_n}$.
539   We'd like a general formula for the term U_n^n. Let's rewrite the previous expressions
540 for $n = 0$, 1 and 2 in a more suggestive way

$$U_n^0 \left|\alpha\right\rangle = 1 \times \left|\alpha\right\rangle, \tag{C.4}$$

$$U_n^1 \left|\alpha\right\rangle = \begin{pmatrix} \cos \delta_n e^{\gamma_n Re(\alpha)} \\ -i \sin \delta_n e^{\gamma_n Re(\alpha)} \end{pmatrix} \begin{pmatrix} \left|(\alpha + \gamma_n)e^{-i\lambda_n}\right\rangle \\ \left|-(\alpha + \gamma_n)e^{-i\lambda_n}\right\rangle \end{pmatrix}, \tag{C.5}$$

$$
U_n^2 \left|\alpha\right\rangle =
\begin{pmatrix}
\cos^2 \delta_n e^{\gamma_n (Re(\alpha) + Re((\alpha+\gamma_n)e^{-i\lambda_n})} \\
-i \sin \delta_n \cos \delta_n e^{\gamma_n (Re(\alpha) + Re((\alpha+\gamma_n)e^{-i\lambda_n})} \\
-i \sin \delta_n \cos \delta_n e^{\gamma_n (Re(\alpha) + Re(-(\alpha+\gamma_n)e^{-i\lambda_n})} \\
-\sin^2 \delta_n e^{\gamma_n (Re(\alpha) + Re(-(\alpha+\gamma_n)e^{-i\lambda_n})}
\end{pmatrix}
\cdot
\begin{pmatrix}
\left|((\alpha+\gamma_n)e^{-i\lambda_n} + \gamma_n)e^{-i\lambda_n}\right\rangle \\
\left|-((\alpha+\gamma_n)e^{-i\lambda_n} + \gamma_n)e^{-i\lambda_n}\right\rangle \\
\left|(-(\alpha+\gamma_n)e^{-i\lambda_n} + \gamma_n)e^{-i\lambda_n}\right\rangle \\
\left|-(-(\alpha+\gamma_n)e^{-i\lambda_n} + \gamma_n)e^{-i\lambda_n}\right\rangle
\end{pmatrix} .
\tag{C.6}
$$

We generalize the previous result for abirtrary n such that we have the multiplication of two vectors of length 2^n:

$$
U_n^n \left|\alpha\right\rangle =
\begin{pmatrix}
b_n^0 \\
b_n^1 \\
\vdots \\
b_n^{2^n-1}
\end{pmatrix}
\begin{pmatrix}
\left|a_n^0\right\rangle \\
\left|a_n^1\right\rangle \\
\vdots \\
\left|a_n^{2^n-1}\right\rangle
\end{pmatrix} ,
\tag{C.7}
$$

where the coefficients are given by a branching recurrence relation given by the base case $b_n^0 = 1$ and $a_n^0 = \alpha$. The recurrences are

$$
a_n^{2k-1} = e^{-i\lambda_n}(a_{n-1}^k + \gamma_n) ,
\tag{C.8}
$$

$$
a_n^{2k} = -e^{-i\lambda_n}(a_{n-1}^k + \gamma_n) ,
\tag{C.9}
$$

$$
b_n^{2k-1} = \cos \delta_n \, b_{n-1}^k e^{\gamma_n Re(a_{n-1}^k)} ,
\tag{C.10}
$$

$$
b_n^{2k} = -i \sin \delta_n \, b_{n-1}^k e^{\gamma_n Re(a_{n-1}^k)} .
\tag{C.11}
$$

C.1 Recurrence in the a vector components

We can rewrite the recurrence in a simpler way to avoid the branching depending on the vector component by using the floor function. Therefore,

$$
a_n^l = e^{i\pi l} e^{-i\lambda_n}(a_{n-1}^{\lfloor l/2 \rfloor} + \gamma_n) .
\tag{C.12}
$$

The base case is $a_0^0 = \alpha$. By simple inspection we see that

$$
a_1^l = e^{i(\pi \lfloor l \rfloor - \lambda_n)}(a_0^{\lfloor l/2 \rfloor} + \gamma_n) = e^{i(\pi \lfloor l \rfloor - \lambda_n)}\alpha + e^{i(\pi \lfloor l \rfloor - \lambda_n)}\gamma_n ,
\tag{C.13}
$$

$$
a_2^l = e^{i(\pi \lfloor l \rfloor - \lambda_n)}(a_1^{\lfloor l/2 \rfloor} + \gamma_n) = e^{i(\pi [\lfloor l \rfloor + \lfloor l/2 \rfloor] - 2\lambda_n)}\alpha + e^{-i\lambda_n}(e^{i\pi \lfloor l \rfloor} + e^{i\pi \lfloor l/2 \rfloor})\gamma_n ,
\tag{C.14}
$$

$$
a_3^l = e^{i(\pi \lfloor l \rfloor - \lambda_n)}(a_2^{\lfloor l/2 \rfloor} + \gamma_n) = e^{i(\pi [\lfloor l \rfloor + \lfloor l/2 \rfloor + \lfloor l/4 \rfloor] - 3\lambda_n)}\alpha + e^{-i\lambda_n}(e^{i\pi \lfloor l \rfloor} + e^{i\pi \lfloor l/2 \rfloor} + e^{i\pi \lfloor l/4 \rfloor})\gamma_n .
\tag{C.15}
$$

Solving this recurrence is nontrivial since it involves a recurrence in two indexes, and it also has non-constant coefficients. Luckily, after many trials, we found a solution by simple inspection:

$$
a_n^l = e^{i(\pi f(n,l) - n\lambda_n)}\alpha + S(n,l)\gamma_n ,
\tag{C.16}
$$

where

$$
f(n,l) \equiv \sum_{k=0}^{n-1} \lfloor l/2^k \rfloor ,
\tag{C.17}
$$

$$
S(n,l) \equiv \sum_{k=1}^{n} e^{i(\pi f(k,l) - k\lambda_n)} ,
\tag{C.18}
$$

C.2 Recurrence in the b vector components

Applying the same logic we used for the previous recurrence, we can write the recurrence equation for b_n^l in a more compact way using the floor function:

$$b_n^l = \frac{e^{-i\delta_n}}{2}(1 + (-1)^l e^{2i\delta_n})b_{n-1}^{\lfloor l/2 \rfloor} e^{\gamma_n Re(a_{n-1}^{\lfloor l/2 \rfloor})} = \frac{e^{-i\delta_n}}{2} G(l) b_{n-1}^{\lfloor l/2 \rfloor} e^{\gamma_n Re(a_{n-1}^{\lfloor l/2 \rfloor})}, \tag{C.19}$$

where $G(l) = 1 + (-1)^l e^{2i\delta_n}$. The base case is $b_0^0 = 1$. By simple inspection we see that

$$b_1^l = \frac{e^{-i\delta_n}}{2} G(l) b_0^1 e^{\gamma_n Re(a_0^{\lfloor l/2 \rfloor})} = \frac{e^{-i\delta_n}}{2} e^{\gamma_n Re(a_0^{\lfloor l/2 \rfloor})}, \tag{C.20}$$

$$b_2^l = \frac{e^{-i\delta_n}}{2} G(l) b_1^{\lfloor l/2 \rfloor} e^{\gamma_n Re(a_1^{\lfloor l/2 \rfloor})} = \frac{e^{-2i\delta_n}}{4} G(\lfloor l \rfloor) G(\lfloor l/2 \rfloor) e^{\gamma_n Re(a_0^{\lfloor l/4 \rfloor} + a_1^{\lfloor l/2 \rfloor})}, \tag{C.21}$$

$$b_3^l = \frac{e^{-i\delta_n}}{2} G(l) b_2^{\lfloor l/2 \rfloor} e^{\gamma_n Re(a_2^{\lfloor l/2 \rfloor})} = \frac{e^{-3i\delta_n}}{8} G(\lfloor l \rfloor) G(\lfloor l/2 \rfloor) G(\lfloor l/4 \rfloor) e^{\gamma_n Re(a_0^{\lfloor l/8 \rfloor} + a_1^{\lfloor l/4 \rfloor} + a_2^{\lfloor l/2 \rfloor})}. \tag{C.22}$$

Let's find a solution to the recurrence. Defining the following function (for which we have not found a closed form):

$$H(n, l) \equiv \frac{e^{-in\delta_n}}{2^n} \prod_{k=0}^{n-1} G(\lfloor l/2^k \rfloor), \tag{C.23}$$

we have

$$b_n^l = H(n, l) \exp\left(\gamma_n Re\left[\sum_{k=0}^{n-1} a_k^{\lfloor l/2^{n-k} \rfloor}\right]\right). \tag{C.24}$$

Let's calculate the term inside the exponential with more detail:

$$\sum_{k=0}^{n-1} a_k^{\lfloor l/2^{n-k} \rfloor} = \alpha\left(\sum_{k=0}^{n-1} e^{i(\pi f(k, \lfloor l/2^{n-k} \rfloor) - k\lambda_n)}\right) + \gamma_n\left(\sum_{k=0}^{n-1} S(k, \lfloor l/2^{n-k} \rfloor)\right). \tag{C.25}$$

Furthermore, let's note that:

$$f(k, \lfloor l/2^{n-k} \rfloor)) = \sum_{j=0}^{k-1} \lfloor l/2^{n-k+j} \rfloor \equiv r(k, l), \tag{C.26}$$

and

$$S(k, \lfloor l/2^{n-k} \rfloor)) = \sum_{j=1}^{k} e^{i(\pi \sum_{i=0}^{j-1} \lfloor l/2^{n-k+i} \rfloor - j\lambda_n)} \equiv T(k, l). \tag{C.27}$$

Then we have

$$\sum_{k=0}^{n-1} a_k^{\lfloor l/2^{n-k} \rfloor} = \alpha\left(\sum_{k=0}^{n-1} e^{i(\pi r(k, l) - k\lambda_n)}\right) + \gamma_n \sum_{k=0}^{n-1} T(k, l). \tag{C.28}$$

Finally, we can define

$$J(n, l) \equiv \sum_{k=0}^{n-1} e^{i(\pi r(k, l) - k\lambda_n)}, \tag{C.29}$$

$$Z(n, l) \equiv \sum_{k=0}^{n-1} T(k, l), \tag{C.30}$$

with which we have

$$\sum_{k=0}^{n-1} a_k^{\lfloor l/2^{n-k} \rfloor} = \alpha J(n,l) + \gamma_n Z(n,l) \,, \tag{C.31}$$

and we therefore conclude that the solution to the recurrence equation for b_n^l is:

$$b_n^l = H(n,l) e^{\gamma_n Re(\alpha J(n,k) + \gamma_n Z(n,l))} \,. \tag{C.32}$$

D Coherent to coherent state amplitudes

One of the noteworthy features of (B.23) is that all of the dependence on the sum index k in the functions H, J, Z, S appears through the features of its dyadic expansion. That is, k is used as an integer number generator via quotients with 2^j. Moreover, it only goes into the result through the value of $e^{i\pi \lfloor l/2^j \rfloor}$, which is always ± 1. That means we are using integer numbers to build binary numbers, or equivalently, sign sequences

$$k \in \mathbb{Z} \text{ s.t. } k < 2^n \iff \{s_\ell\}_{\ell=1}^n(k) = \{s_\ell | s_\ell = e^{i\pi \lfloor k/2^\ell \rfloor}\}. \tag{D.1}$$

Therefore, the sum can be rewritten as a sum over sign choices. Taking the floor function of integers divided by powers of 2 is one way to do this, but any way of generating all possible sign sequences of size n is an equivalent description.

With the correspondence we just outlined, we can write the above functions as

$$S(n,k) = \sum_{\ell=1}^n \left(\prod_{j=0}^{\ell-1} s_j(k) \right) e^{-i\ell\lambda_n}, \tag{D.2}$$

$$H(n,k) = \frac{(-i \sin(\delta_n) \cos(\delta_n))^{n/2}}{(-i \tan(\delta_n))^{\frac{1}{2} \sum_{j=0}^{n-1} s_j(k)}}, \tag{D.3}$$

$$J(n,k) = \sum_{\ell=0}^{n-1} \left(\prod_{j=0}^{\ell-1} s_{n-\ell+j}(k) \right) e^{-i\ell\lambda_n}, \tag{D.4}$$

$$Z(n,k) = \sum_{\ell=0}^{n-1} \sum_{j=0}^{\ell-1} \left(\prod_{i=0}^{j-1} s_{n-\ell+i}(k) \right) e^{-ij\lambda_n}, \tag{D.5}$$

where we have used that

$$\# \text{ of positive signs} = \frac{n + \sum_{j=0}^{n-1} s_j(k)}{2}, \tag{D.6}$$

$$\# \text{ of negative signs} = \frac{n - \sum_{j=0}^{n-1} s_j(k)}{2}. \tag{D.7}$$

Now we may drop the k label altogether and write

$$S_n[s] = \sum_{\ell=1}^{n} \left(\prod_{j=0}^{\ell-1} s_j \right) e^{-i\ell\lambda_n}, \tag{D.8}$$

$$H_n[s] = \frac{(-i\sin(\delta_n)\cos(\delta_n))^{n/2}}{(-i\tan(\delta_n))^{\frac{1}{2}\sum_{j=0}^{n-1} s_j}}, \tag{D.9}$$

$$J_n[s] = \sum_{\ell=0}^{n-1} \left(\prod_{j=0}^{\ell-1} s_{n-\ell+j} \right) e^{-i\ell\lambda_n}, \tag{D.10}$$

$$Z_n[s] = \sum_{\ell=0}^{n-1} \sum_{j=0}^{\ell-1} \left(\prod_{i=0}^{j-1} s_{n-\ell+i} \right) e^{-ij\lambda_n}, \tag{D.11}$$

so that a general transition amplitude can be written as

$$\langle\beta|U_n^n|\alpha\rangle = \sum_{\{s_k\}_{k=0}^{n-1}} H_n[s]\exp\left(\gamma_n\text{Re}\{\alpha J_n[s] + \gamma_n Z_n[s]\}\right)$$

$$\times \langle\beta|e^{-i\omega t}\left(\prod_{k=0}^{n-1} s_k \right)\alpha + S_n[s]\gamma_n\rangle. \tag{D.12}$$

Furthermore, since $\langle\beta|\alpha\rangle = \exp(-[|\alpha|^2+|\beta|^2-2\beta^*\alpha]/2)$, and using that $S_n[s] = e^{-i\omega t}\left(\prod_{j=0}^{\ell-1} s_j\right) J_n^*[s]$, we can get a more explicit expression for the transition amplitude:

$$\langle\beta|U_n^n|\alpha\rangle = \sum_{\{s_k\}_{k=0}^{n-1}} H_n[s]\exp\left(\gamma_n^2 Z_n[s] + \gamma_n\left[\beta^* S_n[s] + \alpha J_n[s]\right]\right)$$

$$\times \exp\left(-\frac{|\alpha|^2 - 2e^{-i\omega t}\left(\prod_{j=0}^{\ell-1} s_j\right)\beta^*\alpha + |\beta|^2}{2}\right). \tag{D.13}$$

One can now rearrange the sum in terms of the accumulated sign variable

$$s_\ell = \prod_{j=0}^{\ell-1} s_j \tag{D.14}$$

with $s_0 = 1$. In this representation, the defining functions become

$$S_n[s] = \sum_{\ell=1}^{n} s_\ell e^{-i\ell\lambda_n}, \tag{D.15}$$

$$H_n[s] = \left(\frac{-i\sin(2\delta_n)}{2} \right)^{n/2} \exp\left(\frac{\ln(i\cot(\delta_n))}{2} \sum_{j=0}^{n-1} s_j s_{j+1} \right), \tag{D.16}$$

$$J_n[s] = S_n^*[s] s_n e^{-i\omega t}, \tag{D.17}$$

$$Z_n[s] = \sum_{\ell=1}^{n-1} \sum_{j=1}^{\ell} s_{n-\ell+j} s_{n-\ell} e^{-ij\lambda_n}, \tag{D.18}$$

which are all at most quadratic in s_j. This means we can interpret this Trotterized time evolution as an Ising model with complex long-range interactions in presence of an inhomogeneous magnetic field. To see this explicitly, first note that we can write

$$\gamma_n^2 Z_n[s] \underset{n\to\infty}{=} \gamma_n^2 \frac{1}{2} \sum_{\ell,j=1}^{n-1} s_j s_\ell e^{-i|j-\ell|\lambda_n}, \tag{D.19}$$

591 where the equality holds only in the limit $n \to \infty$, i.e., up to terms that contribute multi-
592 plicatively to the full amplitude as $e^{1/n}$, and therefore can be neglected. Similarly, we also
593 have

$$\gamma_n \left[\beta^* S_n[s] + \alpha J_n[s] \right] \underset{n \to \infty}{=} \gamma_n \sum_{\ell=1}^{n-1} s_\ell \left[\beta^* e^{-i\ell\lambda_n} + \alpha s_n e^{-i(n-\ell)\lambda_n} \right] . \tag{D.20}$$

594   Put together, these lead to the sum of two expressions alike the partition function of
595 an Ising model with a particular source term, which is different for each spin variable s_n.
596 Then, we have (Eq. (17) in the main text),

$$
\langle \beta | U_n^n | \alpha \rangle \underset{n \to \infty}{=} \left(\frac{-i \sin(2\delta_n)}{2} \right)^{n/2} e^{-\frac{|\alpha|^2 + |\beta|^2}{2}} \left\{ \sum_{\substack{\{s_k\}_{k=1}^{n-1} \\ s_0 = s_n = 1}} e^{\frac{1}{2} \sum_{j,\ell=1}^{n-1} s_j s_\ell K_{j,\ell} + \sum_{\ell=1}^{n-1} s_\ell B_\ell^+ + e^{-i\omega t} \beta^* \alpha} \right.
$$

$$
\left. + \sum_{\substack{\{s_k\}_{k=1}^{n-1} \\ s_0 = -s_n = 1}} e^{\frac{1}{2} \sum_{j,\ell=1}^{n-1} s_j s_\ell K_{j,\ell} + \sum_{\ell=1}^{n-1} s_\ell B_\ell^- - e^{-i\omega t} \beta^* \alpha} \right\} \tag{D.21}
$$

597 where

$$K_{j,\ell} = \delta_{\ell,j+1} \ln(i \cot \delta_n) + \gamma_n^2 e^{-i|j-\ell|\lambda_n} \tag{D.22}$$

$$B_\ell^\pm = \gamma_n \left[\beta^* e^{-i\ell\lambda_n} \pm \alpha e^{-i(n-\ell)\lambda_n} \right] . \tag{D.23}$$

598   These expressions have exactly the form of an Ising model, and their continuum limit
599 is well-defined for all pieces that involve γ_n as a factor, because the sums over j and ℓ can
600 be directly expressed in terms of integrals that involve a continuous version of the sign
601 variables in the sum $s_\ell \to s(x)$. When there is a finite number of sign flips, the conversion
602 can be made directly. In more general cases, one must interpret $s(x)$ as a local average of
603 the "microscopic" s_ℓ variables.
604   The more difficult part to handle, where the continuum limit is not trivially obtained,
605 is the factor that involves δ_n.
606   One way to rearrange the sum in (D.21) is by counting the number of changes of sign
607 in the sequence $\{s_k\}_{k=0}^n$. Let's say that there are m sign flips in a given sequence s. Then,
608 one has

$$H_n[s] = (\cos \delta_n)^{n/2} (-i \tan \delta_n)^m , \tag{D.24}$$

609 which in the limit $n \to \infty$, at fixed $\omega_0 t$, becomes simply $(-i\omega_0 t/n)^m$. The $(1/n)^m$ factor
610 serves the purpose of averaging over all the possible positions where the sign flip in the
611 sequence s was inserted. One can then take the limit $n \to \infty$ and obtain

$$
\langle \beta | U(t) | \alpha \rangle = e^{-\frac{|\alpha|^2 + |\beta|^2}{2}} \sum_{m=0}^{\infty} \frac{(iP\omega_0 t)^m}{m!} \left\langle e^{-g^2 t^2 Z[s] - igt \left[\alpha J[s] + \beta^* s(1) e^{-i\omega t} J^*[s] \right] + \alpha \beta^* s(1) e^{-i\omega t}} \right\rangle_m , \tag{D.25}
$$

612 where the expectation value $\langle \cdot \rangle_m$ represents an average over all possible configurations
613 of $s(x) \in \{-1, 1\}$ such that there are m sign flips. Explicitly, at each fixed m, the average
614 is defined as

$$\langle G \rangle_m = m! \int_0^1 dz_m \int_0^{z_m} dz_{m-1} \dots \int_0^{z_2} dz_1 G(z_1, z_2, \dots, z_m) , \tag{D.26}$$

615 where $\{z_i\}_{i=1}^m$ are the positions at which $s(x)$ flips sign. The functionals $Z[s]$ and $J[s]$ are
616 the continuum counterparts of $Z_n[s]$ and $J_n[s]$:

$$Z[s] = \frac{1}{2} \int_0^1 dx \int_0^1 dy \, s(x)s(y)e^{-i\omega t|x-y|} \tag{D.27}$$

$$J[s] = s(1)e^{-i\omega t} \int_0^1 dx \, s(x)e^{i\omega tx} . \tag{D.28}$$

617 Assuming we have an ordered list of sign flip positions $\{z_i\}_{i=1}^m$, we can write expressions
618 for Z and J at each value of m directly in terms of the sign flip positions:

$$-g^2 t^2 Z[s] = -\frac{4g^2}{\omega^2} \sum_{k=1}^m \sum_{\ell=1}^{k-1} (-1)^{k+\ell} e^{-i(z_k-z_\ell)\omega t} - \frac{2g^2}{\omega^2} \sum_{k=1}^m (-1)^k \left[e^{-iz_k\omega t} - (-1)^m e^{-i(1-z_k)\omega t} \right]$$

$$- \frac{g^2}{\omega^2} \left(1 - (-1)^m e^{-i\omega t} \right) - \frac{2mg^2}{\omega^2} + \frac{ig^2 t}{\omega} \tag{D.29}$$

$$igt J[s] = \frac{g}{\omega} e^{-i\omega t}(-1)^m \sum_{k=0}^m (-1)^k \left(e^{iz_{k+1}\omega t} - e^{iz_k\omega t} \right) . \tag{D.30}$$

619   With this, it is convenient to introduce the functions

$$F_m = \left\langle e^{-g^2 t^2 Z[s] - igt\left[\alpha J[s] + \beta^* s(1)e^{-i\omega t} J^*[s]\right] - \alpha\beta^*\left[1 - s(1)e^{-i\omega t}\right]} \right\rangle_m e^{\frac{2mg^2}{\omega^2} + \left(\alpha + \frac{g}{\omega}\right)\left(\beta^* + \frac{g}{\omega}\right)\left[1 - (-1)^m e^{-i\omega t}\right] - \frac{ig^2 t}{\omega}} . \tag{D.31}$$

620   We extract the prefactor in the second line to isolate the dependence on the sign flips
621 into a single expression. That is to say, we have defined F_m such that $F_0 = 1$, and factorized
622 out all terms that do not depend on the sign flip positions for $m > 0$. To be explicit, in
623 terms of F_m the amplitude reads

$$\langle \beta | U(t) | \alpha \rangle = e^{-\frac{|\alpha|^2 - 2\beta^*\alpha + |\beta|^2}{2}} e^{\frac{ig^2 t}{\omega}} \sum_{m=0}^\infty \frac{(iP\omega_0 t)^m}{m!} e^{-\frac{2mg^2}{\omega^2} - \left(\alpha + \frac{g}{\omega}\right)\left(\beta^* + \frac{g}{\omega}\right)\left[1 - (-1)^m e^{-i\omega t}\right]} F_m , \tag{D.32}$$

624 and F_m is given by

$$F_m = \left\langle \exp\left(-\frac{4g^2}{\omega^2} \sum_{k=1}^m \sum_{\ell=1}^{k-1} (-1)^{k+\ell} e^{-i(z_k-z_\ell)\omega t} - \frac{2g}{\omega} \sum_{k=1}^m \left[\left(\beta^* + \frac{g}{\omega}\right)(-1)^k e^{-iz_k\omega t} \right.\right.\right.$$
$$\left.\left.\left. - \left(\alpha + \frac{g}{\omega}\right)(-1)^{m+k} e^{-i(1-z_k)\omega t} \right] \right) \right\rangle_m \tag{D.33}$$

625 where the average is taken over the possible sign flip positions $z_k \in (0,1)$, with $\{z_k\}_{k=1}^m$
626 an ordered sequence.
627   Equation (D.32), (which corresponds to Eq.(17) in the main text), is a well-defined
628 power series in ω_0, of which one can numerically compute each term.

References

630 [1] W. Heisenberg, Über den anschaulichen inhalt der quantentheoretischen kinematik
631   und mechanik, (On the intuitive content of quantum theoretical kinematics and
632   mechanics), Zeitschrift für Physik **43**(3), 172 (1927), doi:10.1007/BF01397280.

[2] E. Schrödinger, Quantisierung als eigenwertproblem (Quantization as an eigenvalue problem.), Annalen der Physik **384**(4), 361 (1926), doi:https://doi.org/10.1002/andp.19263840404, https://onlinelibrary.wiley.com/doi/pdf/10.1002/andp.19263840404.

[3] L. de Broglie, Recherches sur la théorie des Quanta (Research on the Theory of Quanta.), Theses, Migration - université en cours d'affectation (1924).

[4] A. Einstein, Über einen die erzeugung und verwandlung des lichtes betreffenden heuristischen gesichtspunkt (On a heuristic point of view concerning the production and transformation of light.), Annalen der Physik **322**(6), 132 (1905), doi:https://doi.org/10.1002/andp.19053220607, https://onlinelibrary.wiley.com/doi/pdf/10.1002/andp.19053220607.

[5] N. Bohr, Über die serienspektra der elemente (On the series spectra of the elements.), Zeitschrift für Physik **2**(5), 423 (1920), doi:10.1007/BF01329978.

[6] H. A. Kramers and G. H. Wannier, Statistics of the two-dimensional ferromagnet. part i, Phys. Rev. **60**, 252 (1941), doi:10.1103/PhysRev.60.252.

[7] H. A. Kramers and G. H. Wannier, Statistics of the two-dimensional ferromagnet. part ii, Phys. Rev. **60**, 263 (1941), doi:10.1103/PhysRev.60.263.

[8] P. Jordan and E. Wigner, Über das Paulische Äquivalenzverbot, Zeitschrift fur Physik **47**(9-10), 631 (1928), doi:10.1007/BF01331938.

[9] D. C. Mattis and E. H. Lieb, Exact solution of a many-fermion system and its associated boson field, Journal of Mathematical Physics **6**(2), 304 (1965), doi:10.1063/1.1704281, https://pubs.aip.org/aip/jmp/article-pdf/6/2/304/19083264/304_1_online.pdf.

[10] S. Coleman, Quantum sine-gordon equation as the massive thirring model, Phys. Rev. D **11**, 2088 (1975), doi:10.1103/PhysRevD.11.2088.

[11] S. Mandelstam, Soliton operators for the quantized sine-gordon equation, Phys. Rev. D **11**, 3026 (1975), doi:10.1103/PhysRevD.11.3026.

[12] J. M. Maldacena, The Large N limit of superconformal field theories and supergravity, AIP Conf. Proc. **484**(1), 51 (1999), doi:10.1063/1.59653.

[13] E. Witten, Anti De Sitter Space And Holography (1998), hep-th/9802150.

[14] S. Gubser, I. Klebanov and A. Polyakov, Gauge theory correlators from non-critical string theory, Physics Letters B **428**(1–2), 105–114 (1998), doi:10.1016/s0370-2693(98)00377-3.

[15] H. F. Trotter, On the product of semi-groups of operators, Proceedings of the American Mathematical Society **10**(4), 545 (1959).

[16] I. I. Rabi, On the process of space quantization, Phys. Rev. **49**, 324 (1936), doi:10.1103/PhysRev.49.324.

[17] I. I. Rabi, Space quantization in a gyrating magnetic field, Phys. Rev. **51**, 652 (1937), doi:10.1103/PhysRev.51.652.

[18] E. Ising, Beitrag zur theorie des ferromagnetismus (Contribution to the theory of ferromagnetism.), Zeitschrift für Physik **31**(1), 253 (1925), doi:10.1007/BF02980577.

[19] E. Jaynes and F. Cummings, Comparison of quantum and semiclassical radiation theories with application to the beam maser, Proceedings of the IEEE **51**(1), 89 (1963), doi:10.1109/PROC.1963.1664.

[20] J. H. Eberly, N. B. Narozhny and J. J. Sanchez-Mondragon, Periodic spontaneous collapse and revival in a simple quantum model, Phys. Rev. Lett. **44**, 1323 (1980), doi:10.1103/PhysRevLett.44.1323.

[21] G. Rempe, H. Walther and N. Klein, Observation of quantum collapse and revival in a one-atom maser, Phys. Rev. Lett. **58**, 353 (1987), doi:10.1103/PhysRevLett.58.353.

[22] D. Kleppner, Inhibited spontaneous emission, Phys. Rev. Lett. **47**, 233 (1981), doi:10.1103/PhysRevLett.47.233.

[23] T. Niemczyk, F. Deppe, H. Huebl, E. P. Menzel, F. Hocke, M. J. Schwarz, J. J. Garcia-Ripoll, D. Zueco, T. Hümmer, E. Solano, A. Marx and R. Gross, Circuit quantum electrodynamics in the ultrastrong-coupling regime, Nature Physics **6**(10), 772 (2010), doi:10.1038/nphys1730.

[24] P. Forn-Díaz, J. J. García-Ripoll, B. Peropadre, J. L. Orgiazzi, M. A. Yurtalan, R. Belyansky, C. M. Wilson and A. Lupascu, Ultrastrong coupling of a single artificial atom to an electromagnetic continuum in the nonperturbative regime, Nature Physics **13**(1), 39 (2017), doi:10.1038/nphys3905.

[25] F. Yoshihara, T. Fuse, S. Ashhab, K. Kakuyanagi, S. Saito and K. Semba, Superconducting qubit–oscillator circuit beyond the ultrastrong-coupling regime, Nature Physics **13**(1), 44 (2017), doi:10.1038/nphys3906.

[26] J. Casanova, G. Romero, I. Lizuain, J. J. García-Ripoll and E. Solano, Deep strong coupling regime of the Jaynes-Cummings model, Phys. Rev. Lett. **105**, 263603 (2010), doi:10.1103/PhysRevLett.105.263603.

[27] D. Zueco, G. M. Reuther, S. Kohler and P. Hänggi, Qubit-oscillator dynamics in the dispersive regime: Analytical theory beyond the rotating-wave approximation, Phys. Rev. A **80**, 033846 (2009), doi:10.1103/PhysRevA.80.033846.

[28] S. De Liberato, D. Gerace, I. Carusotto and C. Ciuti, Extracavity quantum vacuum radiation from a single qubit, Phys. Rev. A **80**, 053810 (2009), doi:10.1103/PhysRevA.80.053810.

[29] S. Felicetti, T. Douce, G. Romero, P. Milman and E. Solano, Parity-dependent state engineering and tomography in the ultrastrong coupling regime, Scientific Reports **5**(1), 11818 (2015), doi:10.1038/srep11818.

[30] G. Günter, A. A. Anappara, J. Hees, A. Sell, G. Biasiol, L. Sorba, S. De Liberato, C. Ciuti, A. Tredicucci, A. Leitenstorfer and R. Huber, Sub-cycle switch-on of ultrastrong light–matter interaction, Nature **458**(7235), 178 (2009), doi:10.1038/nature07838.

[31] P. Forn-Díaz, J. Lisenfeld, D. Marcos, J. J. García-Ripoll, E. Solano, C. J. P. M. Harmans and J. E. Mooij, Observation of the bloch-siegert shift in a qubit-oscillator system in the ultrastrong coupling regime, Phys. Rev. Lett. **105**, 237001 (2010), doi:10.1103/PhysRevLett.105.237001.

[32] Y. Yan, Z. Lü and H. Zheng, Bloch-siegert shift of the rabi model, Phys. Rev. A **91**, 053834 (2015), doi:10.1103/PhysRevA.91.053834.

[33] P. Forn-Díaz, G. Romero, C. J. P. M. Harmans, E. Solano and J. E. Mooij, Broken selection rule in the quantum Rabi model, Scientific Reports **6**(1), 26720 (2016), doi:10.1038/srep26720.

[34] D. Braak, Integrability of the rabi model, Phys. Rev. Lett. **107**, 100401 (2011), doi:10.1103/PhysRevLett.107.100401.

[35] D. E. Chang, J. S. Douglas, A. González-Tudela, C.-L. Hung and H. J. Kimble, Colloquium: Quantum matter built from nanoscopic lattices of atoms and photons, Rev. Mod. Phys. **90**, 031002 (2018), doi:10.1103/RevModPhys.90.031002.

[36] P. Saad, S. H. Shenker and D. Stanford, JT gravity as a matrix integral (2019), arXiv:1903.11115.

[37] M.-J. Hwang, R. Puebla and M. B. Plenio, Quantum phase transition and universal dynamics in the rabi model, Physical Review Letters **115**(18), 180404 (2015), doi:10.1103/PhysRevLett.115.180404.

[38] L. Bakemeier, A. Alvermann and H. Fehske, Quantum phase transition in the dicke model with critical and non-critical entanglement, Physical Review A **85**(4), 043821 (2012), doi:10.1103/PhysRevA.85.043821.

[39] M. Suzuki, Generalized trotter's formula and systematic approximants of exponential operators and inner derivations with applications to many-body problems, Communications in Mathematical Physics **51**, 183 (1976).

[40] N. Hatano and M. Suzuki, Finding exponential product formulas of higher orders, In A. Das and B. K. Chakrabarti, eds., Quantum Annealing and Other Optimization Methods, vol. 679 of Lecture Notes in Physics, pp. 37–68. Springer (2005).

[41] A. M. Childs, Y. Su, M. C. Tran, N. Wiebe and S. Zhu, Theory of trotter error with commutator scaling, Physical Review X **11**(1), 011020 (2021).

[42] S. Lloyd, Universal quantum simulators, Science **273**, 1073 (1996).